P8R.6 AN INTEGRATED DISPLAY AND ANALYSIS METHODLOGLY FOR MULTI-VARIABLE RADAR DATA

Brenda A. Dolan* and Steven A. Rutledge
Colorado State University, Fort Collins, Colorado

1. INTRODUCTION

During field experiments, it is necessary to make real time decisions using the available field data to direct aircraft operations, develop radar scanning strategies to best meet the scientific objectives of the project, do project nowcasting, develop scientific insights in the field, etc. These can be difficult tasks, especially for extensive projects involving several aircraft and multiple ground-based sensors. Having too much data available can inhibit operations too, since the scientist may have to take time to interpret many different variables from several radars, and combine them with data from other instruments.

Large field projects in the past, such as the Severe Environmental Storms and Mesoscale Experiment (SESAME) in 1979, the Cooperative Convective Precipitation Experiment (CCOPE) in 1981, the Oklahoma-Kansas Preliminary Regional Experiment for STORM-Central (OK PRE-STORM) in 1985, and most recently, the Mesoscale Alpine Programme (MAP) in 1999, have demonstrated the utility of analyzing real-time radar data for use in directing the scientific objectives of the project as well as in now-casting (Biter and Johnson, 1982; Knight, 1982; Cunning, 1986; Houze et al., 1989; Brown, 1992; Chong et al., 2000). However, interpreting the data from many radar variables, as from polarimetric radars, can be time consuming and requires advanced knowledge by the user (Vivekanandan et al., 1999). Thus, it is useful to extract information from the data and combine it into integrated products such as bulk hydrometeor identification, Doppler-derived winds, and radar mosaics to be viewed in real-time. Methods for real-time analysis and processing of radar data have been developed by Vivekanandan et al. (1999) and Chong et al. (2000) and others. The MountainZebra software system described by James et al. (2000) has been used in recent years at the NCAR S-Pol radar for viewing real-time radar products such as particle identification and dual-Doppler derived winds.

The innovative use and development of real-time data processing algorithms in past field projects has provided motivation and ground work for the development of the software described here. The goal of this study is to develop and integrate radar algorithms currently used in post-processing with meteorological observations to develop a near real-time integrated display and analysis tool for use in nowcasting. The network of radars available along the Front Range of Colorado and Wyoming, coupled with the atmospheric observing systems such as the Denver sounding station and surface observation stations, provide a wealth of meteorological data for scientists. Therefore, an integrated display and analysis methodology to assist in the real-time interpretation and analysis of these data sets would be beneficial to radar scientists working at the CSU-CHILL radar facility.

2. DATA AND ALGORITHMS

a. Front Range Radar Network

There are four S-band Doppler radars located along the Colorado and Wyoming eastern plains front range which were used to develop this methodology: two Weather Surveillance Radar - 1988 Doppler's (WSR-88D) (Denver–KFTG and Cheyenne–KCYS) and two Colorado State University research radars (PAWNEE and CSU–CHILL). The relative locations of these radars are shown in Fig. 1, along with the topography of the region.

b. Data

Level II archive formatted data from the National Weather Service WSR-88D radars was retrieved using Unidata's Local Data Manager (LDM) in association with the Collaborative Radar Acquisition Field Test (CRAFT). The LDM is a collection of cooperating systems which select, capture, manage, and distribute meteorological

**Corresponding author address:* Brenda A Dolan, Colorado State Univ., Department of Atmospheric Science, Fort Collins, CO, 80523-1371; email: bdolan@atmos.colostate.edu

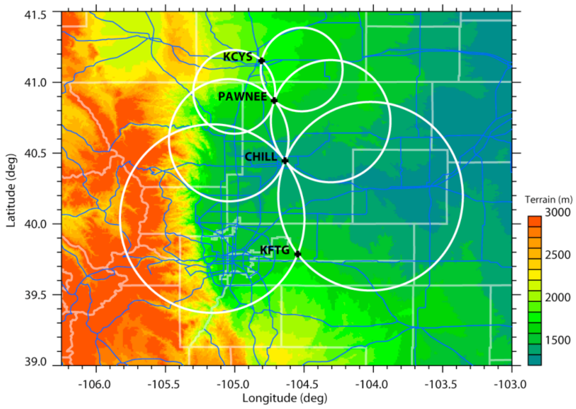

Figure 1: The Front Range Doppler radar network. From top, Cheyenne, WY WSR-88D (KCYS), PAWNEE, CSU-CHILL, and Denver, CO WSR-88D (KFTG). The white circles depict the 30º dual-Doppler beam crossing angles, and the shaded colors indicate the topography of the region in meters. The blue lines indicate major roads and rivers, light grey lines are state and county boundaries.

data products in real-time (http://my.unidata.ucar.edu/content/software/ldm/archive). The CRAFT network is a collaboration between the Center for Analysis and Prediction of Storms (CAPS) program at the University of Oklahoma, Oklahoma State Regents for Higher Education, Unidata, and the University of Washington aimed at gathering NEXRAD data in real-time. Though the data are available almost immediately after a volume scan is completed, there are latency issues with the large size of the files and the number of nodes between the source of the data and the destination computer in the configuration at the CSU-CHILL radar facility.

In addition to radar data, data from the National Weather Service (NWS) Denver sounding was also acquired from the Upper Air Data page on Unisys' weather webpage (http://weather.unisys.com/upper_air). Soundings are obtained twice per day, at 0 and 12 UTC. The file is downloaded to the computer workstation at the CSU-CHILL radar facility as soon as it is available from the website, which can be over an hour after the launch time. In the event data are not available from Unisys, sounding data from the University of Wyoming are used (http://weather.uwyo.edu/upperiar/sounding.html).

During the design and testing phase of this work, data from the PAWNEE radar were not available in real-time. Rather, archived data from the PAWNEE radar were used in lieu of real-time data for developing the software, and data were added to the software later. Data from the CSU-CHILL radar were available immediately after the completion of a volume scan in CHILL raw field data format.

c. Hydrometeor Identification (HID)

The polarimetric capabilities of the CSU-CHILL dual-polarization radar allow for the retrieval of microphysical characteristics of hydrometeors, such as particle size, particle shape, phase, bulk density and particle orientation. It is most useful to combine the radar observables to determine a 'most probable' hydrometeor type as a function of resolution volume. Liu and Chandrasekar (2000) describe a fuzzy logic system which allows for decisions to be made based on overlapping and "noise contaminated" data. Vivekanandan et al. (1999) suggest that the fuzzy logic method for bulk identification of hydrometeors is preferable in real-time to statistical decision trees or neural networks because only simple linear algebraic operations are applied, making the algorithm quick. Additionally, the effects of measurement error do not significantly impact the outcome due to the soft boundaries of the membership beta functions and the weighting functions.

The fuzzy logic hydrometeor identification algorithm (HID) used in this study utilizes a hybrid weighted sum method derived from Lopez and Aubagnac (1997), Carey and Rutledge (1998), Liu and Chandrasekar (2000), Straka et al. (2000), Lim (2001), and Zrnić et al. (2001), and have been adapted to their current form based on input and observations from several sources in the community (K. Wiens, personal communication, 2004). HID uses one dimensional membership beta functions for eleven hydrometeor types: drizzle (Drz), rain (R), wet snow (WS), dry snow (DS), low density (or 'dry') graupel (DG), high density (or 'wet') graupel (WG), small hail (SH), small hail mixed with rain (Sh+r), large hail (LH), large hail mixed with rain (Lh+r), and vertical ice (VI). It also allows for an unclassified category (UC) in the instance when none of the hydrometeor types score a significant truth value. The input variables are horizontal reflectivity (Z), differential reflectivity (Z_{dr}), specific differential phase (K_{dp}), linear depolarization ratio (L_{dr}), and correlation coefficient (ρ_{hv}), and temperature. For the purposes of real-time bulk processing, the temperature profile is derived from the local sounding.

d. Rain rate retrieval

The rain rate, R, at a given point from the radar can be related to the reflectivity, Z, by a general power-law equation (Battan, 1979; Bringi and Chandrasekar, 2001). Since rain rate is proportional to the 3.67th moment of DSD and reflectivity to the 6th moment of DSD, it is readily evident that Z-R relationships are very sensitive to the variability of DSD. The Z-R relationship used by the NWS in the mid-latitudes is:

$$Z=300R^{1.4} \tag{1}$$

Standard Z-R relationships are also problematic due to their sensitivity to calibration, attenuation, beam-blockage, and the presence of hail. Some of the NWS WSR-88D's, such as KFTG, truncate Z at 53 dBZ in order to minimize contamination from hail. This limits the rain rates that can be calculated by the WSR-88D radars to 104 mm hr^{-1}.

Techniques have been developed for rain rate and rainfall estimation using polarimetric information (Chandrasekar et al., 1993; Ryzhkov and Zrnić, 1995; Petersen et al., 1999, and Cifelli et al., 2004). Following the methodology described in Chandrasekar et al. (1993), Cifelli et al. (2004) have developed a polarimetric 'blended algorithm' which uses a decision tree to determine the best estimate of rainfall based on measurement thresholds. The algorithm makes decisions by determining thresholds on the ice fraction, Z_{dr}, K_{dp}, and reflectivity. Based on the thresholds, the best rain rate relationship is selected to minimize ice contamination and bogus data. When reflectivities fall below 30 dBZ, the algorithm reduces to the standard Z-R equation for estimating the rain rate. For a more detailed description, see Cifelli et al. (2004).

Although this technique is still subject to assumptions, studies by Cifelli et al. (2004) and Petersen et al. (1999) have demonstrated that this method for calculating the rain rate, and subsequently the total cumulative rainfall, does at least as well as, if not better than, standard Z-R relationships. Additionally they have verified the output against rain gauge measurements.

e. Dual-Doppler

Four radars located along the Colorado and Wyoming Front Range allow for three dual-Doppler pairs: KCYS and PAWNEE, PAWNEE and CSU-CHILL, and KFTG and CSU-CHILL. For the purposes of this study, the minimum beam-crossing angle was set at 30° (Davies-Jones, 1979). The area enclosed by beam-crossing angles excluding 30° for each dual-Doppler network is outlined in white in Fig. 1.

PAWNEE and CSU-CHILL have been strategically placed as to maximize the dual-Doppler coverage area. The baseline between the two is 48 km, and they are aligned north to south in order to be perpendicular to the average mean flow, maximizing the amount of time a storm spends in the dual-Doppler coverage area. A fourth pair, CSU-CHILL and KCYS, could be considered for a dual-Doppler analysis, but the baseline is nearly 80 km, and the spatial resolution at the farthest points would be almost 2.8 km and therefore was not used for the purposes of this study.

The method for determining the three dimensional wind field from a pair of Doppler radars is described in Armijo (1969) and O'Brien (1970). In this scheme, the anelastic continuity equation is integrated to determine the vertical wind using boundary conditions at the surface and top of the storm, as well as assumptions about the particle fall speed. O'Brien (1970) describes three methods for determining the vertical velocity, w: upward, downward, and variational. These stem from the method of integration of the continuity equation, whether it be ground up (upward), top down to surface (downward), or top down with a redistribution of the error (variational). Downward integration minimizes the residual errors at the surface due to the exponential decrease in density with height (Bohne and Srivastiva, 1975). The downward method was applied in this study.

3. METHODOLOGY

a. Processing Algorithm

Files are first converted to Universal Format (UF), which organizes data in the natural coordinates of the radar (azimuth angle relative to north, elevation angle, and slant range). The WSR-88D level II files are converted to UF using the xltrsii data translator available as part of the SOLOii package developed at the National Center for Atmospheric Research (NCAR). This translator accounts for the different gate spacing for the reflectivity and radial velocity data due to the separate surveillance and Doppler scans at the lowest elevation angles. This is done by reinterpolating the velocity data such that the gate size is the same as the reflectivity gate spacing and storing them into the same sweep structure. This single sweep structure is necessary for use with the NCAR REORDER software package.

CSU-CHILL (henceforth referred to as CHILL) files are first converted to universal format using a translator written by Dave Brunkow, senior engineer at the CSU-CHILL facility. The polarimetric capabilities of the CHILL radar allow for additional editing of the data to remove contamination from anomalous propagation (AP). As described in Ryzhkov and Zrnić (1998), the correlation coefficient (ρ_{hv}) can be used to distinguish between ground clutter and meteorological targets. Additionally, the standard deviation of the differential phase ($SD(\Phi_{dp})$) can be used to filter out non-meteorological echo. Anomalous propagation is especially a problem when calculating rain rates and rainfall accumulations. The appropriate thresholds for non-meteorological returns for the CHILL radar were determined to be $SD(\Phi_{dp})>18°$ and $\rho_{hv}<0.8$. The standard deviation of the phase is calculated at each gate by averaging 21 gates, 10 in front and 10 behind. Thus the CHILL data were 'cleaned-up' using thresholds on the polarimetric variables.

The data were gridded using the REORDER software package developed at NCAR. The software uses a customized grid input file which allows the user to chose the grid definitions based on the storm. However, all data were interpolated to the Cartesian grid using the Cressman weighting scheme (Cressman, 1959). Users can either specify a variable or fixed radius of influence, depending on the location of the storm. Additionally, the volumes are gridded in altitude coordinates above mean sea level (MSL). Grid domains can be specified for each radar. However, considerations for real-time processing limit the size and resolution of the grids.

Storm advection is an integral part of performing a dual-Doppler synthesis, because the storm can evolve substantially within the duration of a volume scan. Therefore, it is important to advect the volume scans to a common time in order to perform the dual-Doppler synthesis. In order to minimize the advection at any one grid point (and the error that could accumulate from that), two volumes are selected for dual-Doppler synthesis only if their volume start times are within three minutes of one another.

Determining the advection direction and speed is a much trickier task. In post analysis, a radar scientist can manually ascertain the speed and direction by looping through volumes throughout the lifetime of an individual storm. In real-time processing, this information must be gathered quickly and for entire grid-domains. This algorithm uses a local sounding to find the 700 mb 'steering winds'. If a sounding is not available, or the scientist notices the mean flow is not represented by the 700 mb winds, the user can manually set default values for the wind speed and direction. Errors in the derived wind field may be introduced when the 700 mb winds or user specified advection parameters are not representative of the true storm motion.

The radial velocities were first locally unfolded using the UNFOLD option in REORDER, then globally unfolded using the NCAR Custom Editing and Display of Reduced Information in Cartesian space (CEDRIC) program (Mohr and Miller, 1983). The two radial velocities are then synthesized at all common grid points using CEDRIC to determine the u, v, and w components of the wind field. The solution of the 3D wind field requires knowledge of the particle fall speed, V_t. Standard V_t-Z relationships are used above and below the melting level, which is either input by the user or determined from the local sounding. The vertical wind is determined using a downward integration method.

The dual-Doppler synthesis can be influenced by the scanning strategy of the WSR-88D radars. When the WSR-88Ds are in precipitation mode, the high elevation angles are sparse, leading to large gaps at high altitudes, and not many winds result from the synthesis. In clear-air mode, there is no coverage of the upper elevation angles.

Due to its string manipulation capabilities, Perl was chosen as the language for the processing algorithm. In real-time mode, the software looks for new files to process, grids the data, then calculates rain rate, hydrometeor identification (in the case of CHILL) and attempts a dual-Doppler synthesis. A simple flow-chart diagram of the real-time algorithm processing is illustrated in Fig. 2.

It was readily apparent that CHILL files would be the quickest available, so the algorithm looks for and processes those first. If a CHILL file is available, the file type is determined and converted to UF appropriately. Then it is run through the program to eliminate clutter via thresholding of the polarimetric variables and calculate K_{dp}. Once this is complete, the volume is gridded to Cartesian coordinates using REORDER. The program then determines if a sounding matches the grid volume time within 12 hours, and if so, uses the sounding temperature profile in the hydrometeor identification. If no sounding is available, the user can specify a melting level and the generated temperature profile will be fixed at 10 ºC below the melting level, 0 ºC at the melting level, and –10 ºC above the melting level. The CSU blended rainfall algorithm is run to find the rain rate, and if the newest volume time is within 2 hours of the previous volume time, it is added to the accumulation. If not, then a new rainfall accumulation is started. The final output is in netCDF format, which is sent to the visualization program as soon as the processing is complete.

The algorithm then proceeds through the other three radars, checking for new files. If a new files exists and it is not in universal format (UF), it is converted to UF via the translation software. If it is a WSR-88D file, a check is performed to determine if the radar was in precipitation mode or clear-air mode. If it was in clear-air mode, the file is archived without processing. If it is in precipitation mode, then it is matched against processed files for dual-Doppler pairs. If a matching file for the dual-Doppler pair exists within 3 minutes, the algorithm checks against sounding files to determine if the advection can be extracted from the sounding or if default values should be used. If a sounding exists within 12 hours, the 700 mb winds are used for the advection speed and direction; if not user input values are used. The matching files are gridded using REORDER, then the velocities are globally unfolded using CEDRIC, and finally the 3D wind field is derived from the two radial velocities using CEDRIC. The final step is to run a comparison rain rate and rainfall algorithm. Once this process is complete, the files are sent to the visualization software and archived in the appropriate directory. If a dual-Doppler synthesis is not possible, the radar volume is gridded to Cartesian coordinates and run through the rainfall and rain rate algorithms before being sent to the visualization software. In addition to the visualization software, images can be published to the web for display in real-time.

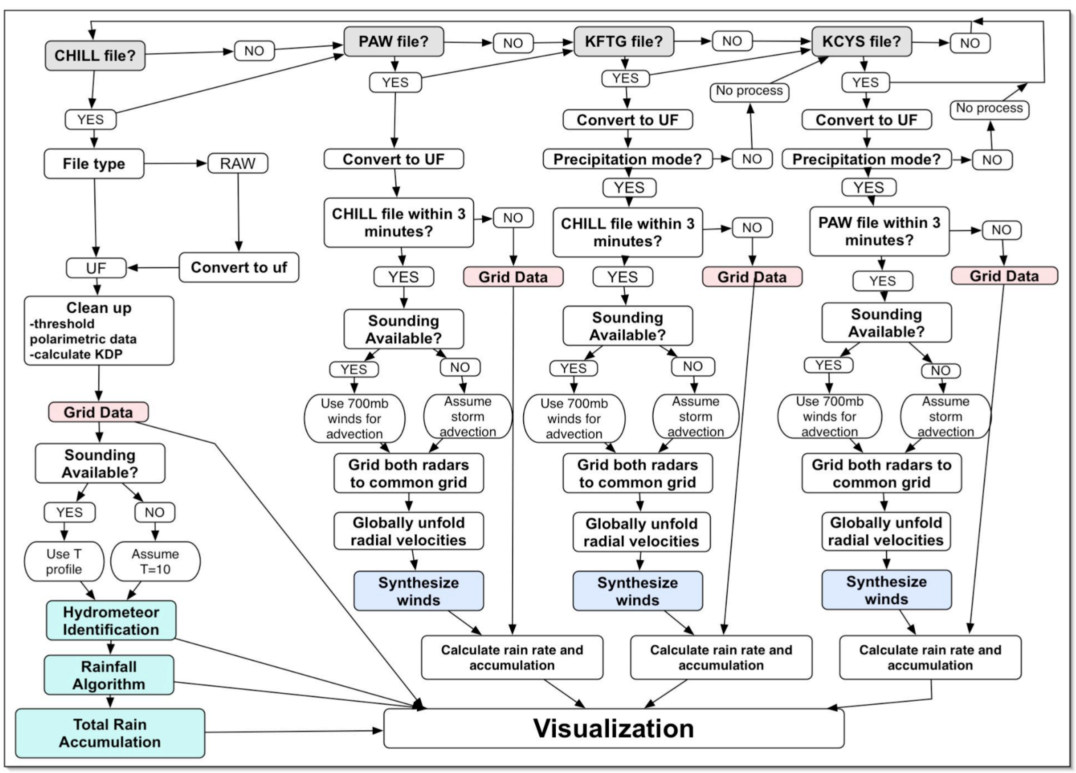

Figure 2: Flow chart of the integrated display and analysis tool for multi-variable radar data processing in real-time.

b. Visualization

Research Systems Inc. (RSI)'s IDL was chosen as the programming language for the visualization software. The visualization software can operate in real-time mode where it continually updates as new files become available from the processing software. The display consists of two windows, a mosaic panel and an image panel with four configurable plots. The user can choose the radar, variable, and height in each image panel as well as activate overlays such as county lines, roads and dual-Doppler winds and multiple contour variables. The image panel configuration can be changed to include vertical cross sections and zoom in on a storm (Fig. 3). The mosaic panel can be configured to display either reflectivity or rain rate, with the combined dual-Doppler winds overlaid. Additionally, the user can save images for archival or post-processing.

The mosaic is created by combining the data from all available radar data. Grid points are first filled in with CHILL data, then with KFTG and KCYS data. PAWNEE data is not used in either the reflectivity or rain rate mosaic, due to excessive clutter in the mountains. Figure 4 illustrates an example of a reflectivity mosaic at 2216 UTC on 09 June 2005. The dual-Doppler winds from each of the three dual-Doppler pairs can be overlaid on the mosaic, and can be color-coded by dual-Doppler pair. The mosaic is a useful way to get an overall view of the echoes along the Front Range.

Although the display offers similar radar products to software packages that have been available in the past, it is unique in several ways. First of all, the user can display data from multiple radars simultaneously, as well as specify the grid size, resolution, and origin for the processing of the data. This functionality could be useful in situations where one specific storm is the focus of the real-time studies. A high resolution grid domain restricted around the storm could provide detailed information about that specific cell without requiring the processing time involved with gridding the entire radar domain, while the mosaic provides an overview of much of the Front Range. However, since the original UF files are archived, scientists can process them at a future time on a different grid. Secondly, the display software

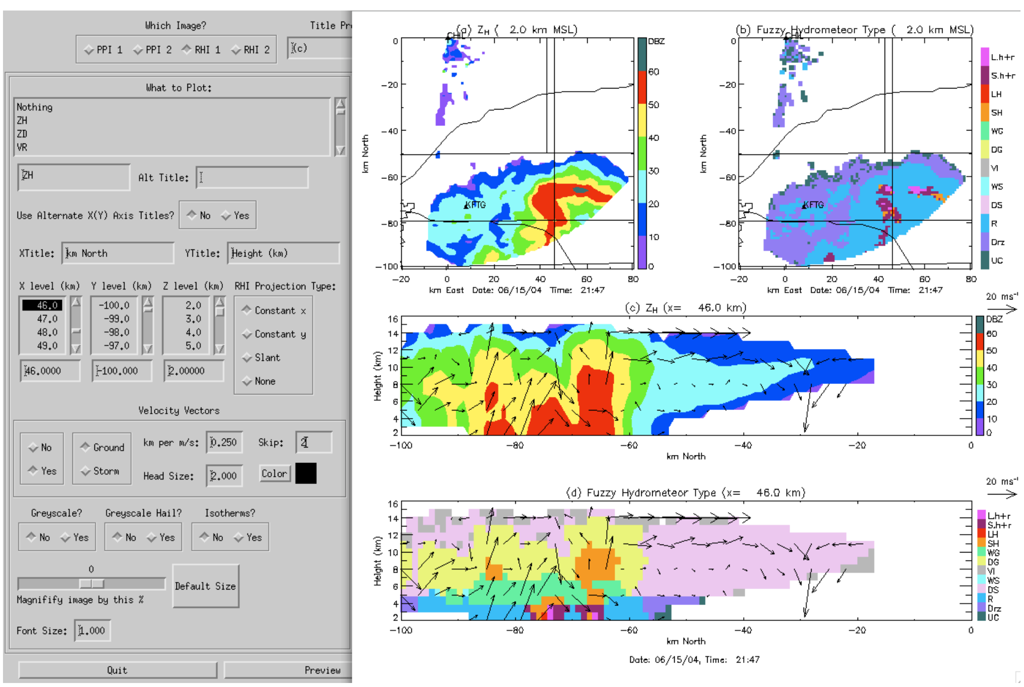

Figure 3: An example of the User Interface for the real-time display tool. The control panel to the right illustrates the expanded options for configuring images. Here, the user has selected to view two vertical cross-sections as well as two Constant Altitude Planned Position Indicator (CAPPI) plots. Data is from 15 June 2004 at 2147 UTC. a) reflectivity and b) hydrometeor type from CHILL data at 2.0 km MSL, c) reflectivity and d) hydrometeor identification vertical cross sections at x=46.0 km from CHILL with dual-Doppler winds from a synthesis with KFTG.

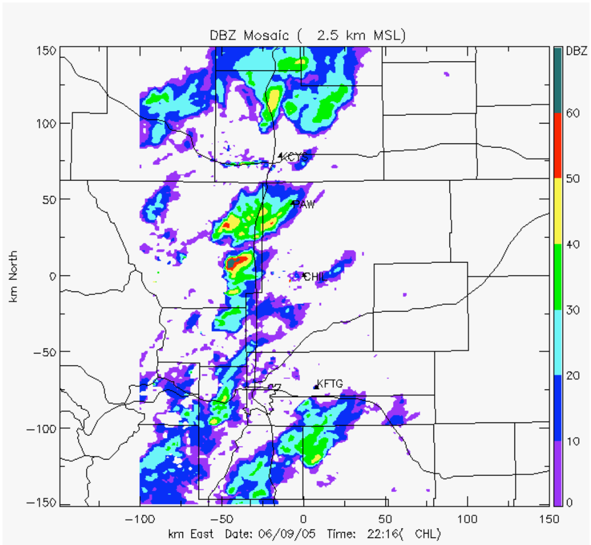

Figure 4: Reflectivity mosaic made from CHILL, KFTG and KCYS data at 2.5 km MSL. CHILL data are from 2216 UTC, KFTG data are from 2217 UTC, and KCYS data are from 2216 UTC. Data were combined by filling in the grid points successively beginning with CHILL data, then KFTG data in the southern half of the grid (y < 0 km) and KCYS data in the northern half of the grid (y > 0 km).

allows the user the flexibility to change the window configuration, display data from several different radars with contouring and overlays, and zoom in and out of the grid. Users can also change the color scale and display range for each variable. The print function permits the user to save particularly interesting images and mosaics for analysis at a later time. The flexibility available in this algorithm results in a unique tool for the processing and display of data from multiple Doppler radars.

4. CASE STUDY: 09 JUNE 2005

On the afternoon of 09 June 2005, a strong storm passed over Fort Collins, Colorado producing hail as large as 44 mm (1.75”). Due to the interesting wind features, ground reports of large hail, and the locality of the storm, this case is particularly well-suited to demonstrate the capabilities of the software described in this paper.

During the 9 June 2005 event, the CHILL and PAWNEE radars were running coordinated 5 minute volume scans, often coinciding with the start time of the KFTG WSR-88D. CHILL performed sector scans for 16 elevation angles every 5 minutes beginning at 2201 UTC, and PAWNEE ran 360° full volume scans for 14-16 elevation angles. Coordinated scans with KFTG began at 2201 UTC. The KFTG WSR-88D was running the Volume Coverage Pattern (VCP) 11, or “Severe Weather Precipitation Mode”, which is a 5 minute scan containing 14 elevation sweeps. The KCYS radar was scanning using the new VCP 12, which is similar to VCP 11, but covers 14 elevation angles in 4.1 minutes.

Figure 5 shows a reflectivity swath of CHILL data from 2100-2259 UTC (LT=UTC-6 hr). The swath was made by taking the highest reflectivity at each grid point in the reflectivity column over the two hour period. The storm that produced hail in Fort Collins (labeled ‘FNL’ in the figure) began in northern Boulder county around 2130 UTC and moved to the northeast at approximately 13 ms^{-1}. Reflectivities in the cell exceeded 60 dBZ for much of the period from 2159 to 2227 UTC. A second pair of cells developed to the west of Fort Collins around 2128 UTC, moving more slowly to the east-northeast. These cells eventually merged with the southern storm north of Fort Collins and died out as it moved into the eastern plains.

Local storm reports from the Boulder NWS Forecast office indicated hail started at 2212 UTC in southwest Fort Collins and continued through 2231 UTC in northwest Fort Collins. Hail reports indicated sizes ranging from 19 mm (0.75”) to 44 mm (1.75”). The local storm reports are marked with an ‘H’ on Fig. 5, with the relative size of the ‘H’ corresponding to relative size of the hail report[1].

The surface environment on 12 UTC was characterized by relatively cool temperatures and weak northerly flow (Fig. 6). The synoptic analysis indicates a low pressure in the southeast corner of Colorado, with a warm front draped through Kansas. The 12 UTC sounding (Fig. 7) shows a small inversion capped by a dry adiabatic layer. Low-level winds were weak out of the north-northwest, with stronger mid- and upper-level flow from the south west.

Scientists at CHILL were able to use the software to observe many aspects of these multi-cellular storms as they evolved. Figure 8 shows a4-panel image plot from 2227 UTC. The top panels are horizontal cross-sections of CHILL

[1] The software does not currently display hail and tornado reports in real-time. Future versions of the software will allow the user the ability to enter the latitude and longitude coordinates of a given severe weather report to be overlaid on the plots.

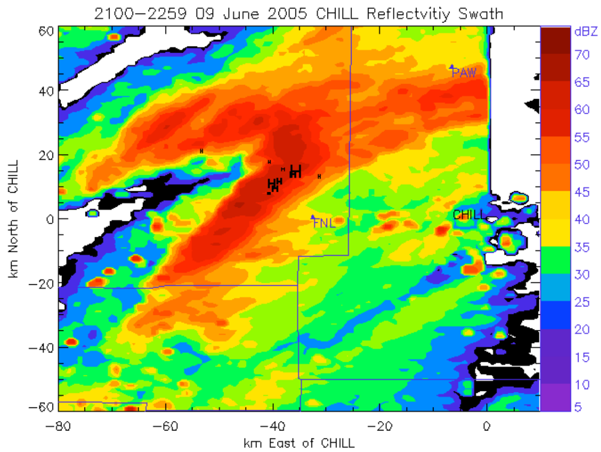

Figure 5: Reflectivity swath for the period between 2100-2259 UTC on 09 June 2005. Reflectivity is from CHILL data. The 'H's indicate location of hail reports; the relative size of the letter corresponds to the relative size of the hail, which ranged from 19 mm (0.75") to 44 mm (1.75"). The swath was created by taking the highest reflectivity value at each grid point over the 2 hr period. 'FNL' indicates the location of the Fort Collins ASOS.

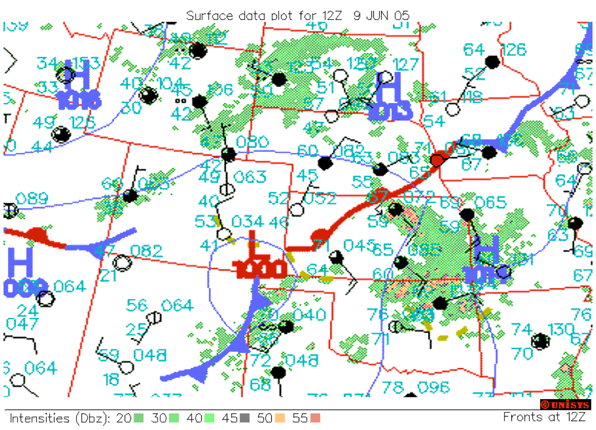

Figure 6: Surface data analysis for 12 Z on 09 June 2005. The winds in northern Colorado are out of the north, and the surface temperatures are in the high 40's °F. From http://weather.unisys.com.

reflectivity and HID at 2.5 km MSL (~1.0 km above ground level). The bottom two panels are vertical cross-sections through the storm at x=-38.0 km of CHILL reflectivity and HID with wind vectors derived from a dual-Doppler synthesis between CHILL and PAWNEE radars. The hail reports from 2226 UTC and 2229 UTC are indicated by the black 'H' on Fig. 8. The HID algorithm indicates a region of large hail, large hail mixed with rain, and small hail mixed with rain collocated

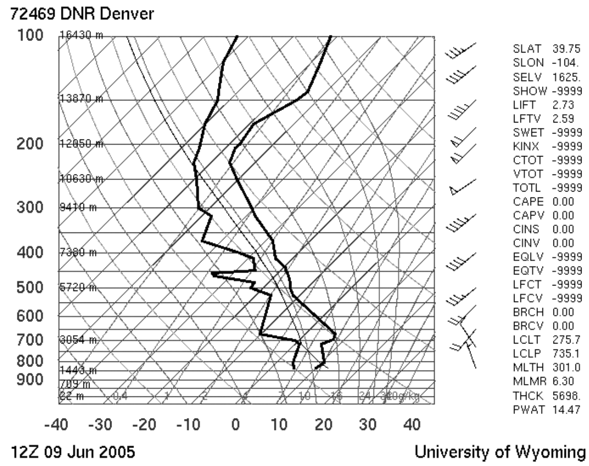

Figure 7: The NWS Denver sounding for 12 UTC on 09 June 2005.

with the strongest reflectivities. There is also a small area of large and small hail south southwest of the PAWNEE radar. Outside of these convective cores, there is a broad domain of rain and drizzle. Surface observations of hail correspond reasonably well with the locations of large hail mixed with rain identified by the HID algorithm. The vertical cross-sections reveal strong winds in a tilted updraft. The winds in the updraft reached 24 ms^{-1}. The vertical cross-section of HID shows both large and small hail in the core of the updraft, surrounded by regions of wet and dry graupel, which is to be expected. The outflow at the top levels of the storm is toward the north.

The data from multiple radars at 2227 UTC showed a large area of discrepancy between the NEXRAD Z-R derived rain rates associated with the storm and the rain rates calculated using the polarimetric data from CHILL. This is indicated in Fig. 9, which shows horizontal cross-sections at 2.5 km MSL for CHILL reflectivity, HID, the CSU blended algorithm rain rate, and the rain rate from KCYS using the standard mid-latitude Z-R relationship. Rain rates calculated from the KCYS radar were greater than 100.00 mm/hr in the core of the storm, whereas the blended algorithm used on the CHILL data show much lower rain rates. This difference is also apparent in the smaller storm to the south southwest of PAWNEE. Comparisons with HID at the same time indicate the presence of large and small hail, which are likely contaminating the Z-R based rain rate estimate. In contrast, the blended algorithm can

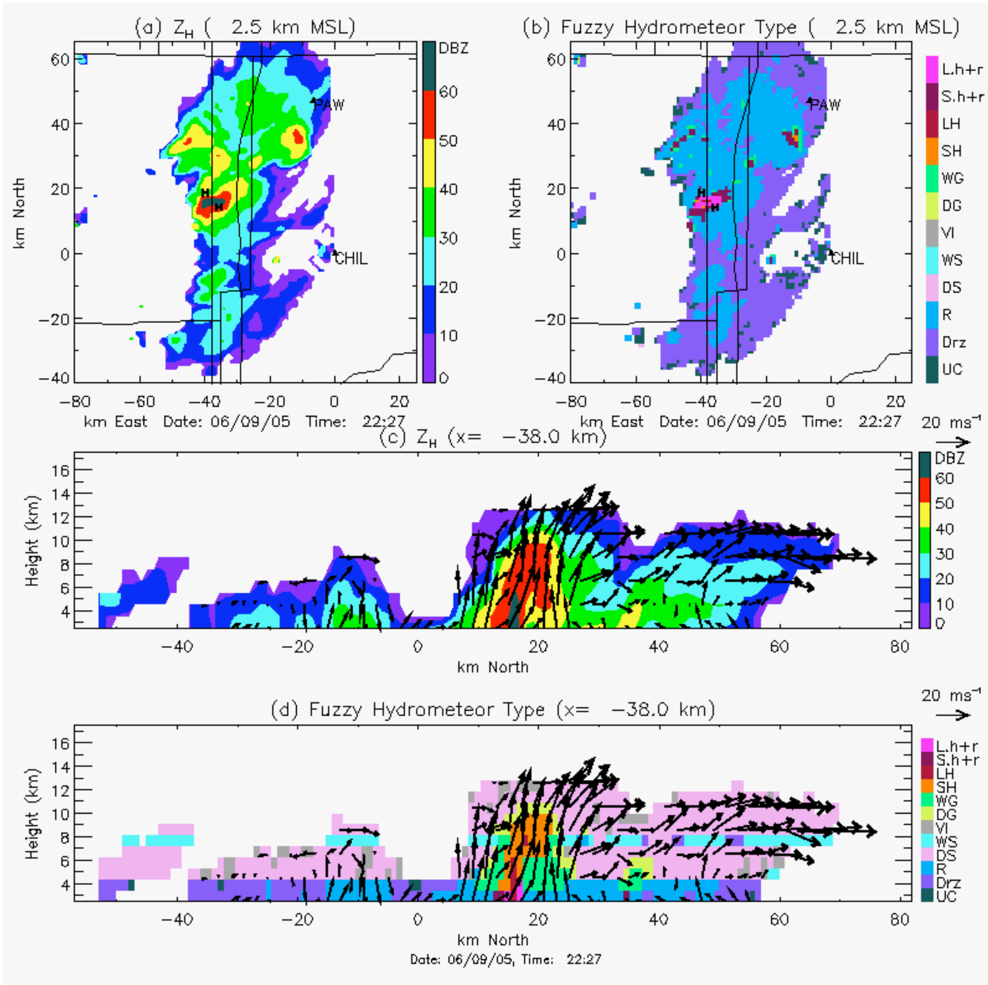

Figure 8: Example of a 4-panel image plot of CHILL data on 09 June 2005 at 2227 UTC. Panels a and b are horizontal cross-sections at 2.5 km MSL of a) reflectivity and b) hydrometeor type. Panels c and d are vertical cross-sections at x=-38.0 km with wind vectors from a synthesis between CHILL and PAWNEE radial velocities overlaid on c) reflectivity and d) hydrometeor type. The black 'H' on panels a and b denote the locations of two hail reports at 2226 UTC (southeast) and 2229 UTC (northwest).

utilize the phase information, which is relatively insensitive to precipitation ice.

The multi-cellular storms moved through the western lobes of all three dual-Doppler pairs described in Section 2e, allowing for a unique look at the storm with four radars and three wind-syntheses. Of particular interest was the observation of an anti-cyclonic rotation in the winds at the lowest levels. The anti-cyclonic turning of the winds was first noted at 2150 UTC and persisted through 2257 UTC at 2.5, 3.5 and 4.5 km MSL. By 2257 UTC the 2.5 km winds were predominately from the north northwest. The clockwise rotation was evident in the wind synthesis between all three dual-Doppler pairs, as well as the CHILL raw radial velocity field. Figure 10 shows an example of the ground-relative wind field at 2227 UTC overlaid on a reflectivity mosaic. The three wind vector colors represent the different dual-Doppler pair syntheses. The red wind vectors are from a synthesis of CHILL and PAWNEE radial velocity, the green vectors are from a KFTG and CHILL synthesis, and the purple vectors are from PAWNEE and KCYS synthesis. Although the exact nature of the anti-cyclone has not been determined, it appears to be topographically forced, possibly a manifestation of the Cheyenne ridge anticyclone, which is characterized by cold, northerly flow off the Cheyenne ridge along the Colorado and Wyoming border (Davis, 1997).

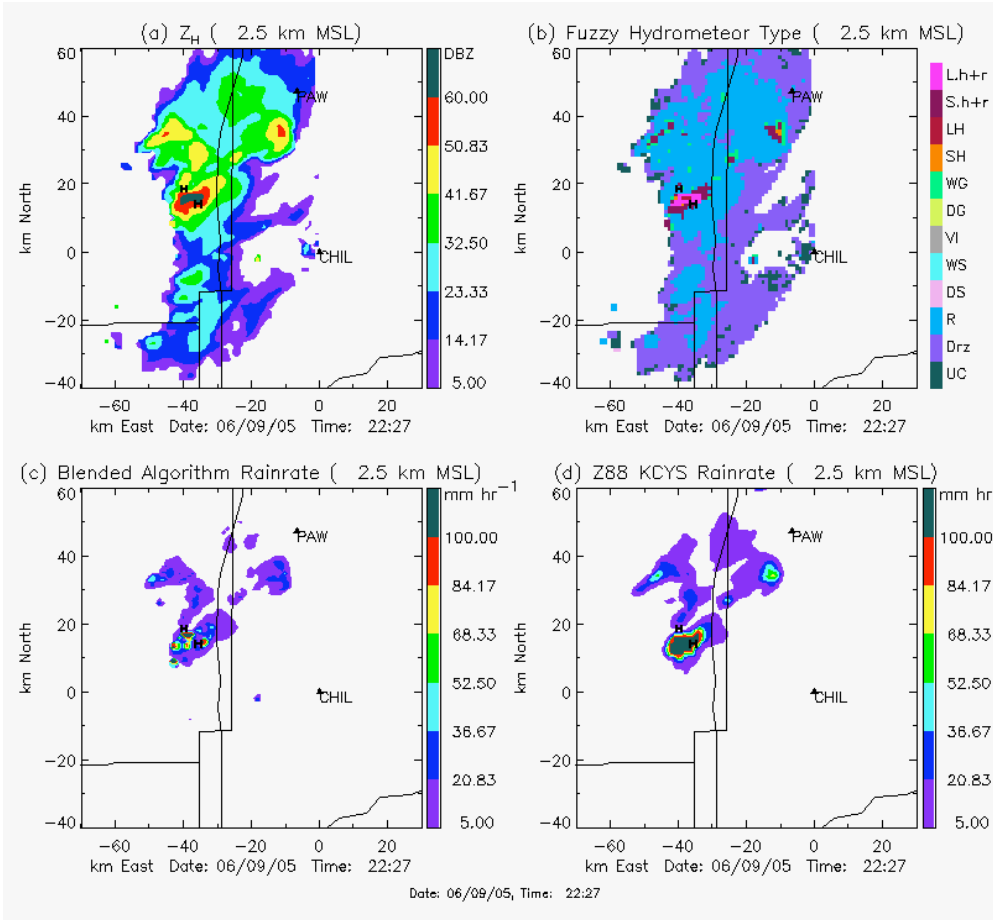

Figure 9: Example of a 4-panel image plot of multiple radar data on 09 June 2005 at 2227 UTC. Panels are horizontal cross-sections at 2.5 km MSL of a) CHILL reflectivity, b) CHILL hydrometeor type, c) rain rate derived from the CHILL blended algorithm, and d) rain rate calculated from KCYS reflectivity data using a Z-R relationship. The black 'H' on panels a and b denote the locations to two hail reports at 2226 UTC (southeast) and 2229 UTC (northwest).

This case also illustrates one of the problems with processing dual-Doppler winds in a bulk sense in quasi-realtime. The advection direction and speed used for the synthesis were derived from the 700 mb winds from the 12 UTC Denver sounding indicating a speed of 3.1 ms^{-1} from 230°. However, a hand analysis of the storm motion shows the storm motion for the southern storm was 13 ms^{-1} at 215°, while the northern storm was moving approximately 4 ms^{-1} from 250°. This discrepancy between the actual storm motions and the advection used from the 'mean' wind could cause errors in the synthesis if the volumes from the two radars were a sufficiently long time apart. However, in this case, three of the four radars were coordinated to begin the volumes within one minute of each other. Therefore this is not too much of a concern for this case, but should be a consideration for future work.

5. CONCLUSIONS

Radars have been used for decades to observe precipitation and other weather phenomena. Advancements such as Doppler and dual-polarization capabilities have greatly increased the amount of information that can be retrieved for scientific insights about storms. Over the years, scientists have continued to develop new ways of combining radar data from multiple radars, as well as other observing platforms, to achieve efficient and insightful methods of viewing the vast amount of data in real-time. Hydrometeor identification using polarimetric measurements has become available during various field projects in

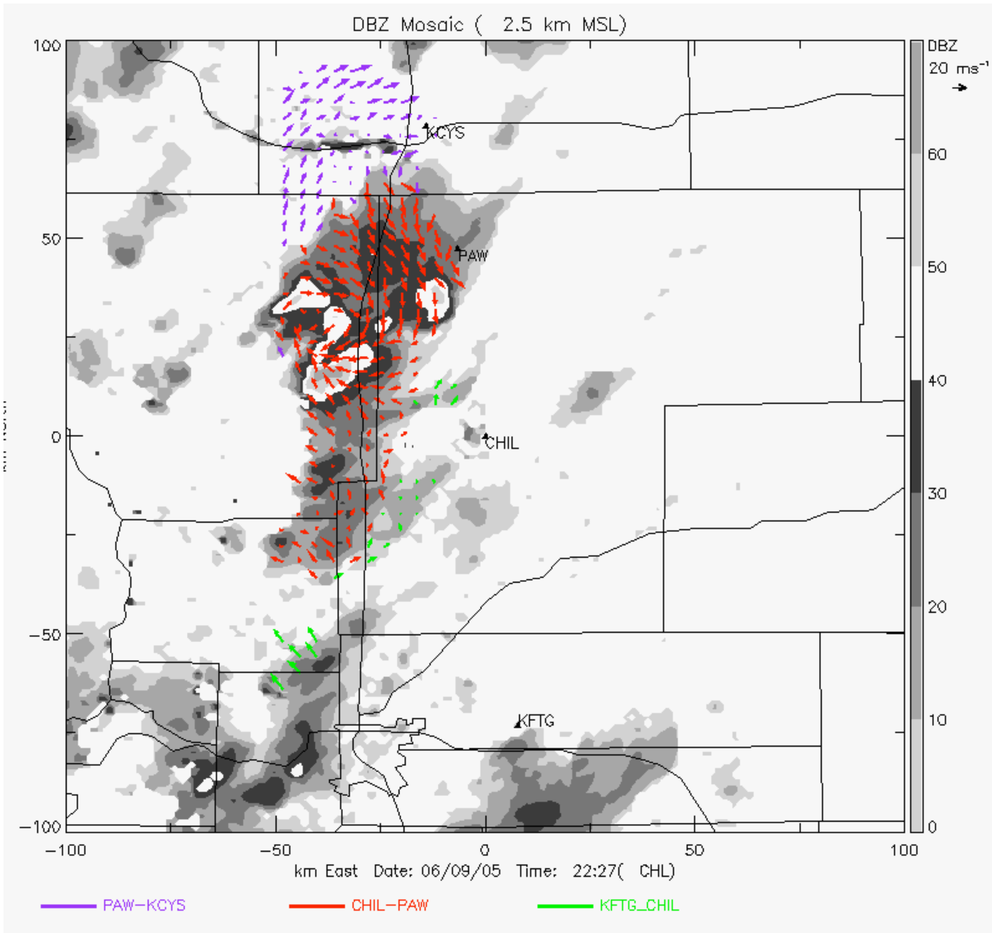

Figure 10: Example of mosaic panel of reflectivity (grayscale) and dual-Doppler derived winds for 2227 UTC on 09 June 2005. The red winds are from a synthesis between CHILL and PAWNEE, the purple winds are from a synthesis between KCYS and PAWNEE, and the green winds are from a synthesis between KFTG and CHILL. Note the anti-cyclonic circulation in the winds just north of the reflectivity center.

recent years, adding to the data available for studying microphysical characteristics. In general though, having multiple platforms available for field projects also presents significant challenges to studying and analyzing the data in real-time to guide field operations (Chong et al., 2000).

Motivated by what has been available in previous projects, the goal of this work was to design and test a real-time analysis and display tool for the four radars along the Colorado and Wyoming Front Range. The analysis tool combines reflectivity and velocity data from CSU-CHILL, PAWNEE, and the KCYS and KFTG WSR-88D radars, as well as the polarimetric data provided by CSU-CHILL, to derive products such as hydrometeor identification, rain rate, total rainfall, wind field, and data mosaics in real-time in a common, user-friendly display format.

The algorithm and display were tested during the summers of 2004 and 2005 at the CSU-CHILL radar facility. Derived products were available within 15 minutes after the beginning of the radar volume scan, with CHILL data being the most ‘real-time’, as it was available within three minutes of a scan volume. Dual-Doppler winds took the longest to acquire (15 minutes after the WSR-88D volume scan), in part due to the time required to download the large files from Unisys’ Local Data Manager. Although the data were not real-time in an instantaneous sense, the software still provided important information for characterizing storms throughout their lifetime. The suite of radar products available with the interactive display software allowed scientists to visualize updraft locations and strengths, determine hydrometeor types present at both the surface and upper-levels of the storm, and identify characteristics in the wind field such as mesocyclones. Comparisons could also be made between radars, revealing differences in the rain rate estimation techniques used by CHILL and WSR-88D.

This study found that a real-time analysis and display tool proved a valuable resource for analyzing and visualizing copious amounts of data from several radars succinctly and efficiently. The software developed for this project provided scientists with numerous options to process and view data from Doppler and polarimetric radars without requiring prior knowledge of the intricacies related to the interpretation of radial velocity and polarimetric variables. Future field experiments, especially those in which a primary objective of CHILL is to direct aircraft, will greatly benefit from such software.

Future work needs to be focused in two major areas: 1) improvements to the software algorithm in terms of both the functionality and the processing and 2) continued testing in the field.

There has already been feedback regarding improvements that can be made to the functionality of the algorithm and display tool. It was apparent during the field testing phase that a loop of the last hour of data would be a useful addition to assist in the analysis of storm development and motion. In terms of the user interface, interest in satellite and surface data overlays has been expressed, as well as lightning data and possibly rain gauge data. With respect to the processing of data, a storm tracking algorithm similar to that used by the National Weather Service would be a better method for determining storm advection information for dual-Doppler analysis. The melting level could be determined using the radar data instead of the local sounding, resulting in better estimates of the actual environment present in the storm. A stratiform and convective partitioning algorithm could be useful in hydrometeor identification to assist in the elimination of unlikely hydrometeor types under certain conditions, and could also be useful in viewing real-time data.

Acknowledgements: The authors would like to thank Dr. Kyle Wiens for his assistance with the display widget and IDL expertise. Paul Hein provided help with the computer aspects of the study. Natalie Tourville and Dennis Flanigan assisted in working with the NEXRAD level II data. Dr. Rob Cifelli, Dr. Larry Carey, Dr. Walt Petersen, Pat Kennedy and Dave Brunkow supported this project with discussions about different aspects of the data processing and interpretation, as well as providing portions of code for the processing algorithms. Pat Kennedy and Bob Bowie collected data during the testing phase of this project. This research was funded primarily by the NSF Information Technology Research grant ATM-0121546 awarded to Colorado State University. This work was supported in part by the Engineering Research Centers Program of the National Science Foundation under NSF Award Number 0313747.

REFERENCES

Armijo, L., 1969: A theory for the determination of wind and precipitation velocities with Doppler radars. *J. Atmos. Sci.,* **26,** 570-575.

Battan, L.J., 1973: *Radar Observations of the Atmosphere.* University of Chicago Press, 324pp.

Biter, C. J., and P.N. Johnson, 1982: Sunday Creek –The CCOPE operations center. *Bull. Am. Meteorol. Soc.*, **63**, 482-486.

Bohne, A. R., and R. C. Srivastava, 1975: Random errors in wind and precipitation fall speed measurement by a triple Doppler radar system. Univ. of Chicago, Tech. Report No 37, 50pp.

Bringi, V.N., and V. Chandrasekar, 2001: Polarimetric Doppler Weather Radar: Principles and Applications, Cambridge University Press, Cambridge, United Kingdom, 636pp.

Brown, Rodger, A., 1992: Initiation and Evolution of Updraft Rotation within an Incipient Supercell Thunderstorm. *J. Atmos. Sci.*, **49**, 1997-2014.

Carey, L. D., and S. A. Rutledge, 1998: Electrical and multiparameter radar observations of a severe hailstorm. *J. Geophys. Res.,* **103**, 13979-14000.

Chandrasekar, V., E. Gorgucci, and G. Scarchilli, 1993: Optimization of multi-parameter radar estimates of rainfall. *J. Appl. Meteor.,* **32**, 1288-1293.

Chong, M., J.-F. Georgis, O. Bousquet, S. R. Brodzik, C. Burghart, S. Cosma, U. Germann, V. Gouget, R. A. Houze Jr., C. N. James, S. Prieur, R. Rotunno, F. Roux, J.

Vivekanandan, and Z.-X. Zeng, 2000: Real-time wind synthesis from Doppler radar observations during the mesoscale alpine programme. *Bull. Am. Meteorol. Soc.,* **81**, 2953-2962.

Cifelli, R., D. Barjenbruch, D. Brunkow, L. Carey, C. Davey, N. Doesken, C. Gimmestad, T. Huse, P. Kennedy, and S. A. Rutledge, 2004: Evaluation of an operational polarimetric rainfall algorithm. AMS 31st Conference on Radar Meteorology, Seattle, WA, 6-12 August 2003.

Cressman, G. P., 1959: An operational objective analysis system. *Mon. Wea. Rev.,* **87,** 367-374.

Cunning, John. B., 1986: The Oklahoma-Kansas Preliminary Regional Experiment for STORM-Central. *Bull. Am. Meteorol. Soc.*, **67**, 1478-1486.

Davis, C. A., 1997: Mesoscale anticyclonic circulations in the lee of the central Rocky Mountains. *Mon. Wea. Rev.*, **125**, 2838-2855.

Davies-Jones, R.P., 1979: Dual-Doppler radar coverage area as a function of measurement accuracy and spatial resolution. *J. Appl, Meteor.,* **18**, 1229-1233.

Houze, R. A. Jr., S. A. Rutledge, M. I. Biggerstaff, and B. F. Smull, 1989: Interpretation of Doppler weather radar displays of midlatitude mesoscale convective systems. *Bull. Am. Meteorol. Soc.*, **70**, 608-619.

James, C. N., S. R. Brodzik, H. Edmon, R. A. Houze Jr., and S. E. Yuter, 2000: Radar data processing and visualization over complex terrain. *Wea. Forecasting,* **15**, 327-338.

Knight, C.A., Ed., 1982: the Cooperative Convective Precipitation Experiment (CCOPE), 18 May-7August 1981. *Bull. Am. Meteorol. Soc.*, **63**, 386-398.

Lim, Sanghun, 2001: Fuzzy logic for hydrometeor classification from polarimetric radar measurements. Master's thesis, Colorado State University, Department of Electrical and Computer Engineering, 97pp.

Liu, H., and V. Chandrasekar, 2000: Classification of hydrometeors based on polarimetric radar measurements: Development of fuzzy logic and neuro-fuzzy systems, and in situ verification. *J. Atmos. Oceanic Tech.,* **17,** 140-164.

Lopez, R. E., and J. P. Aubagnac, 1997: The lightning activity of a hailstorm as a function of changes in its microphysical characteristics inferred from polarimetric radar observations. *J. Geophys. Res.*, ***102,*** 16799-16813.

Mohr, C. G., and L. J. Miller, 1983: CEDRIC – A software package for Cartesian space editing, synthesis and display of radar fields under interactive control. *Preprints, 21st Conf. On Radar Meteorology,* Boston, *Amer. Meteor. Soc.,* 569-574.

O'Brien, J.J., 1970: Alternative solutions to the classical vertical velocity problem. *J. Appl. Meteor.,* **9,** 197-203.

Petersen, W. A., L. D. Carey, S. A. Rutledge, J. C. Knievel, N. J. Doesken, R. H. Johnson, T. B. McKee, T. Vonder Haar and J. F. Weaver, 1999: Mesoscale and radar observations of the Fort Collins Flash Flood of 28 July 1997. *Bull. Amer. Meteorol. Soc.,* **80,** 191-216.

Ryzhkov A. V., and D. S. Zrnić, 1995: Comparison of Dual-Polarization radar estimators of rain. *J. Atmos. Oceanic Tech.*, 12, 249-256.

Ryzhkov, A. V., and D. S. Zrnić, 1998: Polarimetric Rainfall Estimation in the Presence of Anomalous Propagation. *J. Atmos. Oceanic Tech.*, **15**, 1320-1330.

Straka, J. M., D. S. Zrnić, and A. V. Ryzhkov, 2000: Bulk hydrometeor classification and quantification using polarimetric radar data: Synthesis of relations. *J. Appl. Meteor.*, **39**, 1341-1372.

Vivekanandan, J., D.S. Zrnić, S.M. Ellis, R. Oye, A. V. Ryzhkov, and J. Straka, 1999: Cloud microphysics retrieval using S-band dual-polarization radar measurements. *Bull. Am. Meteorol. Soc.,* **80**, 381-388.

Zrnić, D.S., A. Ryzhkov, J. Straka, Y. Liu, and J. Vivekanandan, 2001: Testing a procedure for automatic classification of hydrometeor types. *J. Atmos. Oceanic Tech.*, **18**, 892-913.